

# Density functional theory and *ab initio* molecular dynamics study of NO adsorption on Pd(111) and Pt(111) surfaces

Zhen-Hua Zeng,<sup>1</sup> Juarez L. F. Da Silva,<sup>2</sup> and Wei-Xue Li<sup>1</sup><sup>1</sup>*State Key Laboratory of Catalysis and Center for Theoretical and Computational Chemistry, Dalian Institute of Chemical Physics, Chinese Academy of Sciences, Dalian 116023, China*<sup>2</sup>*Instituto de Física de São Carlos, Universidade de São Paulo, Caixa Postal 369, São Carlos 13560-970, SP, Brazil*

(Received 20 August 2009; revised manuscript received 8 January 2010; published 4 February 2010)

The origin of the unique geometry for nitric oxide (NO) adsorption on Pd(111) and Pt(111) surfaces as well as the effect of temperature were studied by density functional theory calculations and *ab initio* molecular dynamics at finite temperature. We found that at low coverage, the adsorption geometry is determined by electronic interactions, depending sensitively on the adsorption sites and coverages, and the effect of temperature on geometries is significant. At coverage of 0.25 monolayer (ML), adsorbed NO at hollow sites prefer an upright configuration, while NO adsorbed at top sites prefer a tilting configuration. With increase in the coverage up to 0.50 ML, the enhanced steric repulsion lead to the tilting of hollow NO. We found that the tilting was enhanced by the thermal effects. At coverage of 0.75 ML with  $p(2 \times 2)$ -3NO(fcc+hcp+top) structure, we found that there was no preferential orientation for tilted top NO. The interplay of the orbital hybridization, thermal effects, steric repulsion, and their effects on the adsorption geometries were highlighted at the end.

DOI: [10.1103/PhysRevB.81.085408](https://doi.org/10.1103/PhysRevB.81.085408)

PACS number(s): 68.43.Bc, 68.43.Fg, 68.35.Md

## I. INTRODUCTION

Molecular adsorption on transition-metal (TM) surfaces is a common phenomenon on a large number of surface technological processes including catalytic reactions,<sup>1</sup> and an atom-level understanding of the adsorption are required for better activity and functions.<sup>2</sup> Among other, the identification of the adsorbate structures and sites, bond strength are crucial. For diatomic molecules, such as carbon monoxide (CO) and nitride oxide (NO), the possible adsorption sites on close-packed (111) surfaces are top sites, bridge sites, fcc, and hcp hollow sites. Depending on the adsorption sites and coverage, the adsorbed molecules prefers either an upright configuration or tilting configuration with respect to the substrate, as found both experimentally and theoretically.<sup>3–12</sup>

Recent experimental studies (at temperature of 100–300 K) for NO/Pd(111) and NO/Pt(111) at high coverage found that independent on the adsorption sites (top and hollow), all adsorbed NO molecules were tilted.<sup>13–15</sup> For example, in  $c(4 \times 2)$ -2NO(fcc+hcp)/Pd(111) structure, adsorbed NOs were tilted by about 8°, which were attributed to the repulsive lateral interactions.<sup>13</sup> Although recent DFT calculations support this conclusions, the difference between calculated and measured tilted angle is significant.<sup>16</sup> For top NO in  $p(2 \times 2)$ -3NO(fcc+hcp+top) structure, the measured tilting angle at  $T \leq 140$  K is about 5°–10° larger than the calculated values.<sup>10–14,17</sup> The difference between DFT calculations at absolute zero and measurements at finite temperatures indicates possible thermal effects on geometries, which has not been addressed in literature. Moreover, it was found that tilted top NO may point toward different directions, namely, fcc, hcp, or bridge sites nearby.<sup>10–14,17</sup> The physics underlined remains elusive. To shed lights on these problems, we performed DFT calculations at absolute zero and *ab initio* molecular dynamics (MD) simulations at finite temperatures for NO/Pd(111) and NO/Pt(111) in present work.<sup>13</sup>

## II. METHOD

The DFT calculations at 0 K and *ab initio* MD simulations at different temperatures were performed using the generalized gradient approximation formulated by Perdew-Burke-Ernzerhof functional (GGA-PBE),<sup>18</sup> and the all-electron projected augmented wave (PAW) method,<sup>19–21</sup> as implemented in the Vienna *Ab initio* Simulation Package (VASP).<sup>22,23</sup> Plane-wave cut-off energies of 400 and 300 eV were used for the DFT and MD calculations, respectively. For the Brillouin-zone integration, we used  $\Gamma$ -centered ( $6 \times 6$ ) and ( $7 \times 6$ ) **k**-point grids for the  $p(2 \times 2)$  and  $c(4 \times 2)$  unit cells. All calculations were carried out at the optimized lattice constant of bulk Pd ( $a_0=3.95$  Å) and Pt ( $a_0=3.99$  Å), whose differences with experiment are 1.5% and 1.8%.<sup>24</sup> The (111) surfaces were modeled by the repeated four layers slab separated by a vacuum region of 11.40 Å. Test calculations using thicker slabs (for instance seven layers slab) shows that four layers slab are sufficient. The adsorbates were added only one side of the slab, and the dipole corrections were employed to screen the artificial interaction through the vacuum region.

The DFT calculations at coverage of 0.25, 0.50, and 0.75 ML were considered. Adsorbed NOs were placed initially at high symmetry sites (top, fcc, and hcp) and no symmetry constraints were applied during the optimization and MD simulation. The calculations were terminated when the residual forces less are than 0.01 eV/Å. The rotation barriers for adsorbed NO molecules were calculated using the nudge elastic band (NEB) method.<sup>25–28</sup> For MD simulations, a time step of 2 fs was used. The MD simulations were performed up to 30 ps at experimental temperatures of 140, 245, and 300 K for NO/Pd(111) and 300 K for NO/Pt(111).

## III. RESULTS AND DISCUSSIONS

### A. DFT calculations at $T=0$ K

DFT calculations for NO/Pd(111) were performed at coverages of 0.25, 0.50, and 0.75 ML at absolute zero. Calculations

lated average adsorption energy for NO adsorption on the surfaces,  $E_{\text{ad}}$ , was defined by

$$E_{\text{ad}} = (E_{\text{tot}}^{\text{NO/Pd(111)}} - E_{\text{tot}}^{\text{Pd(111)}} - N \times E_{\text{tot}}^{\text{NO}})/N, \quad (1)$$

where  $E_{\text{tot}}^{\text{NO/Pd(111)}}$ ,  $E_{\text{tot}}^{\text{Pd(111)}}$ , and  $E_{\text{tot}}^{\text{NO}}$  are the total energies of NO/Pd(111), clean Pd(111), and NO in gas phase, respectively.  $N$  is the number of adsorbed NO in the unit cell. The energetic most favorable structures identified are:  $(2 \times 2)$ -1NO(fcc) (0.25 ML),  $c(4 \times 2)$ -2NO(fcc+hcp) (0.50 ML), and  $p(2 \times 2)$ -3NO(fcc+hcp+top) (0.75 ML), as indicated in Fig. 1. Calculated  $E_{\text{ad}}$  are  $-2.34$ ,  $-2.03$ , and  $-1.71$  eV, respectively. It can be seen that adsorption energy decreases with the increase in coverage, by about 0.30 eV from 0.25 to 0.50 ML, and another 0.32 eV from 0.50 to 0.75 ML. The variation indicates that there is a pronounced lateral repulsion between adsorbates.<sup>16</sup> Important structural parameters are given in Table I

From Fig. 1 and Table I, we can see that NO in the hollow sites at 0.25 ML prefers an upright configuration, while NO in the top sites (less favorable by 0.82 eV) is tilted by about  $47.7^\circ$  with respect to the normal direction of the surface. At 0.50 ML, however, hollow NO becomes tilted by about  $5^\circ$  due to the lateral repulsion between adsorbed NO. To see this

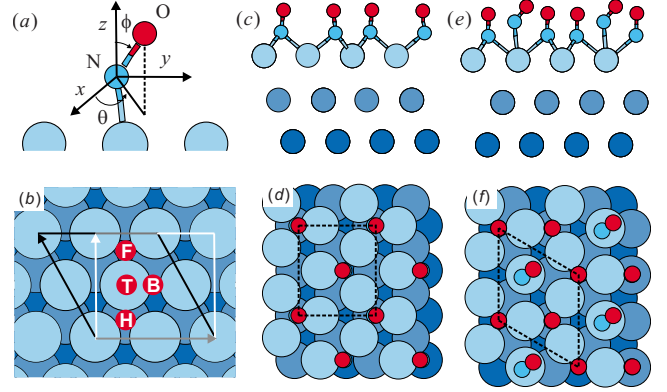


FIG. 1. (Color online) (a) Side view of NO adsorption on Pd(111) surfaces, in which the tilting azimuth angle  $\phi$  and in-plane angle  $\theta$  are indicated; (b) top view of high symmetry adsorption sites ( $F$ : fcc,  $H$ : hcp,  $T$ : top, and  $B$ : bridge) and super cell [black and gray line for  $(2 \times 2)$ , gray and white line for  $c(4 \times 2)$ ] used in calculations; [(c) and (e)] side and [(d) and (f)] top view of  $c(4 \times 2)$ -2NO(fcc+hcp) and  $(2 \times 2)$ -3NO(fcc+hcp+top), respectively.

clearly, we constrained two hollow NO molecules at the upright configuration and optimized other freedoms. The calculated total energy is 89 meV/ $c(4 \times 2)$  higher than the fully

TABLE I. Structural parameters for NO adsorption on Pd(111) at different coverages [fcc and top NO in a  $(2 \times 2)$  supercell at 0.25 ML,  $c(4 \times 2)$ -2NO(fcc+hcp) at 0.50 ML and  $(2 \times 2)$ -3NO(fcc+hcp+top) at 0.75 ML] and different temperatures. The averaged values from the experiments of Ref. 13 for  $c(4 \times 2)$ -2NO(fcc+hcp) at 245 K and  $(2 \times 2)$ -3NO(fcc+hcp+top) at 140 K are given for comparison.

Cover. (ML)	Sites	Cond.	$d_{\text{N-O}}$ (Å)	$d_{\text{N-Pd}}$ (Å)	$\alpha_{\perp\text{-N-O}}$ (deg)	
0.25	fcc	0 K	1.218	2.04	0.0	
		300 K	$1.218 \pm 0.004$	$2.06 \pm 0.03$	$7.3 \pm 3.8$	
		top	0 K	1.181	1.91	47.7
0.50	fcc	0 K	1.213	2.07	5.9	
		245 K	$1.213 \pm 0.004$	$2.09 \pm 0.04$	$9.0 \pm 4.6$	
		300 K	$1.213 \pm 0.006$	$2.09 \pm 0.04$	$9.1 \pm 4.5$	
	expt.	1.22	2.01	8		
	hcp	0 K	1.210	2.08	5.3	
		245 K	$1.211 \pm 0.003$	$2.09 \pm 0.04$	$9.4 \pm 4.7$	
300 K		$1.211 \pm 0.005$	$2.10 \pm 0.04$	$9.6 \pm 4.7$		
expt.	1.23	2.02	8			
0.75	fcc	0 K	1.215	2.08	0.7	
		140 K	$1.215 \pm 0.003$	$2.09 \pm 0.02$	$4.6 \pm 2.4$	
		300 K	$1.216 \pm 0.005$	$2.09 \pm 0.04$	$6.4 \pm 3.3$	
		expt.	1.27	2.02	7	
		hcp	0 K	1.211	2.09	1.3
			140 K	$1.212 \pm 0.002$	$2.09 \pm 0.02$	$4.8 \pm 2.5$
	300 K		$1.212 \pm 0.005$	$2.10 \pm 0.04$	$6.9 \pm 3.6$	
	expt.		1.21	2.07	4	
	top		0 K	1.179	1.93	42.6
			140 K	$1.179 \pm 0.002$	$1.94 \pm 0.03$	$42.7 \pm 4.1$
		300 K	$1.179 \pm 0.002$	$1.95 \pm 0.05$	$42.5 \pm 5.2$	
	expt.	1.16	1.86	47		

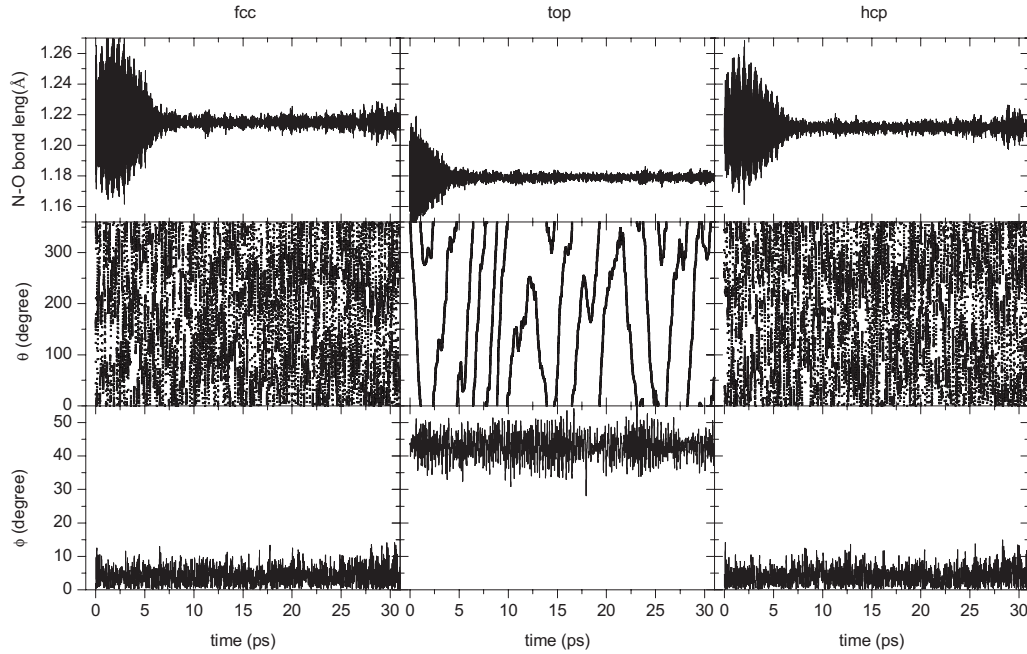


FIG. 2. The evolution of geometrical parameters N-O bond length, the tilting azimuth angle  $\phi$  and in-plane angle  $\theta$  defined in Fig. 1 during MD simulation at 140 K for  $(2 \times 2)$ -3NO(fcc+hcp+top)/Pd(111).

optimized tilted one. This indicates that the tilting of hollow NO in  $c(4 \times 2)$  come from intrinsic lateral repulsion between adsorbates. It should be noticed that the tilting angle ( $5^\circ$ ) calculated at absolute zero remains smaller than the experimental values ( $8^\circ$ ) performed at 245 K. As shown in following MD simulations, the difference comes from the effect of temperature, which were not included in present DFT calculations. At higher coverage of 0.75 ML, calculated tilting angle for top NO ( $42.6^\circ$ ) and hollow NO ( $2^\circ$ ) is smaller than those at 0.25 and 0.50 ML, respectively. This is because of the enhanced steric repulsion at 0.75 ML, which prevents the large tilting. Furthermore, we found slight preference for orientation of the top NO tilting towards the neighbor sites, and calculated energetics for the top NO tilting towards the bridge sites is nearly same with that tilting towards the hollow sites, as reported in previous works.<sup>11,13,17</sup> In fact, the energy barrier for the in-plane rotation of top NO was calculated to be less than 5 meV. This indicates that there is no preferential tilting orientation for top NO at this coverage.

The electronic structure analysis (see details in Ref. 16) shows that the chemical bonding between adsorbed NO and Pd substrates at 0.25 ML was determined by the hybridization between NO  $5\sigma/2\pi^*$  orbitals and Pd  $4d$  bands via so-called donation and back-donation mechanism. The extent of donation and back donation are site dependent and are more extensive for NO adsorption at high coordination (three-fold hollow) sites than that at top sites. This leads to a stronger bonding between hollow NO and Pd substrate and preference of the upright configuration. For top NO, the upright configuration is however energetically unfavorable by 0.39 eV than the tilted one. The energy gain from tilting comes from the enhanced back donation from Pd  $d$  bands to NO  $2\pi^*$  orbitals. Moreover, we found that the work function changes upon NO adsorption are site dependent too. For NO adsorbed in the hollow sites, work function increases by about

0.25 eV, while it decreases by 0.27 eV for NO in the top sites at 0.25 ML. The different sign of the work function change indicates an opposite direction for the adsorption induced dipole moment for hollow and top NO molecules. Correspondingly, at coverage of 0.50 ML [ $c(4 \times 2)$ -2NO(fcc+hcp)], both fcc and hcp NO have same direction of the dipole moment, electrostatic repulsion is developed, which lead to the hollow NO tilted.

### B. Effect of temperature studied by *ab initio* MD simulations

To address the effect of temperature on the structures, *ab initio* MD simulations were performed at temperatures of 140, 245, and 300 K, respectively. Typical simulation time were 30 ps, which is sufficient to reach the equilibrium, as plotted in Fig. 2. In Table I, the average geometric parameters (e.g. bond lengths and tilting angles) and corresponding root-mean-square deviation (RMSD) for various configurations taken from the last 20 ps are summarized.

The effect of temperature can be easily seen for fcc NO at 0.25 ML. In contrast to the upright configuration for hollow NO at  $T=0$  K, for example, we found it tilts by  $7.3 \pm 3.8^\circ$  at 300 K. The effect of temperature was also found in the variation in bond lengths. In this context, we note that the N-O bonding strength ( $E_b=7.3$  eV) is about 5 eV stronger than NO-Pt bond, hence the effect of temperature on N-O bond [ $d_{N-O}$ ] stretching would be modest, compared to that of N-Pd bond [ $d_{N-Pd}$ ] stretching, as indeed found from MD simulation. From Table I, we can see that  $d_{N-O}$  is little affected by temperature, while  $d_{N-Pd}$  increases by 0.02 Å with a RMSD of  $\pm 0.03$  Å. Similar trends are also observed at higher coverages.

For  $c(4 \times 2)$ -2NO(fcc+hcp) at 0.50 ML, MD simulations were carried out at 245 K in order to compare directly with recent experiments performed at same temperature.<sup>13</sup> We found that the tilting angles for NO in the fcc and hcp sites

TABLE II. Structural parameters for NO adsorption on Pt(111) at different coverages [fcc and top NO in a  $(2 \times 2)$  supercell at 0.25 ML,  $(2 \times 2)$ -2NO(fcc+top) at 0.50 ML and  $(2 \times 2)$ -3NO(fcc+hcp+top) at 0.75 ML] at 0 and 300 K.

Cover. (ML)	Sites	Cond.	$d_{\text{N-O}}$ (Å)	$d_{\text{N-Pt}}$ (Å)	$\alpha_{\perp\text{-N-O}}$ (deg)
0.25	fcc	0 K	1.224	2.10	0.0
		300 K	$1.230 \pm 0.006$	$2.11 \pm 0.05$	$5.0 \pm 4.0$
0.50	top	0 K	1.181	1.91	47.7
		300 K	$1.182 \pm 0.007$	$1.98 \pm 0.03$	$50.2 \pm 2.9$
	fcc	0 K	1.232	2.10	0.3
		300 K	$1.231 \pm 0.007$	$2.09 \pm 0.03$	$5.5 \pm 2.9$
0.75	top	0 K	1.182	1.98	50.2
		300 K	$1.182 \pm 0.002$	$1.97 \pm 0.05$	$48.9 \pm 5.9$
	fcc	0 K	1.224	2.11	1.3
		300 K	$1.224 \pm 0.008$	$2.10 \pm 0.03$	$5.9 \pm 3.3$
	hcp	0 K	1.214	2.13	1.3
		300 K	$1.215 \pm 0.006$	$2.13 \pm 0.04$	$6.7 \pm 3.6$
top	0 K	1.184	1.97	45.3	
	300 K	$1.184 \pm 0.002$	$1.96 \pm 0.04$	$44.5 \pm 4.3$	

increase from  $5.9^\circ$  and  $5.3^\circ$  at  $T=0$  K to  $9.1 \pm 4.5^\circ$  and  $9.4 \pm 4.7^\circ$  at 245 K, respectively. The effects of temperature is significant. More important, the calculated results including the effect of temperature agree better with experimental measurements ( $8^\circ$ ).

For  $p(2 \times 2)$ -3NO(fcc+hcp+top) at 0.75 ML, NO molecules in the fcc and hcp sites with tilting angle of  $2^\circ$  at 0 K increases to  $4.6 \pm 2.4^\circ$  and  $4.8 \pm 2.5^\circ$  at 140 K,  $6.4 \pm 3.3^\circ$  and  $6.9 \pm 3.6^\circ$  at 300 K, respectively. In addition to see the effect of temperature on the tilting angle and RMSD, this result shows further that the effect increases with temperatures. For top NO, the effect of temperature is however modest: the tilting angle of top NO is  $42.6^\circ$  at  $T=0$  K and becomes  $42.7^\circ$  and  $42.5^\circ$  at 140 and 300 K. Compared to the measured angle of  $47^\circ$  for top NO at 0.75 ML,<sup>13</sup> calculated value is about  $4^\circ$  smaller. This difference may come from the underestimation of the gap between NO  $5\sigma$  and  $2\pi^*$  orbitals due the employment of the semilocal exchange-correlation functional.<sup>10</sup> Indeed, the calculation at 0 K using hybrid functional HSE06 (Ref. 29) with better description of the gap between NO  $5\sigma$  and  $2\pi^*$  orbital shows that the tilting angle for top NO at 0.25 ML increases to  $51.3^\circ$ , compared to  $47.7^\circ$  calculated by PBE.

The findings of the intrinsic electronic effect and thermal effect as well as their interplay on the geometries found for NO/Pd(111) applies to NO adsorption on other TM surfaces too. To illustrate this, we present the results for NO adsorption on Pt(111), and main results are given in Table II. At 0.25 ML, as found in NO/Pd(111), hollow NO prefers an upright configuration at 0 K, and becomes tilted with angle of  $5.0 \pm 4.0^\circ$  at 300 K. At high coverage of 0.75 ML with same configuration as Pd(111)[ $p(2 \times 2)$ -3NO(fcc+hcp+top)],<sup>10,12,14,30</sup> the effect of temperature on geometries are essential same as NO adsorption on Pd(111).

For NO adsorption on Pt(111) at intermediate coverage of 0.50 ML, the picture is slightly different from NO/Pd(111) due to different configurations formed. Contrast to  $c(4$

$\times 2)$ -2NO(fcc+hcp) on Pd(111), the energetically favorable configuration formed on Pt(111) is  $p(2 \times 2)$ -2NO(fcc+top). This structure is formed because the small difference of adsorption energy between hollow and top NO on Pt(111) (0.33 eV) than that on Pd(111) (0.82 eV). Formation of  $p(2 \times 2)$ -2NO(fcc+top) configuration on Pt(111) allows to minimize the site competition and electrostatic repulsion. This is however unlikely for NO adsorption on Pd(111), in which top NO is highly energetically unfavorable.<sup>10,16</sup>

For  $p(2 \times 2)$ -2NO(fcc+top)/Pt(111), top NO is also tilted too. Compared to tilted top NO on Pd(111)/Pt(111) at 0.75 ML with no preferential tilting direction, top NO on Pt(111) at 0.50 ML prefers to tilt towards the fcc sites nearby, and calculated barrier for its in-plane rotation over hcp sites using NEB is 60 meV [Fig. 3(b)]. This can be seen from explicit MD simulation at 300 K, as shown in Fig. 3(a). From this figure, it is clear that adsorbed NO tends to stay in a

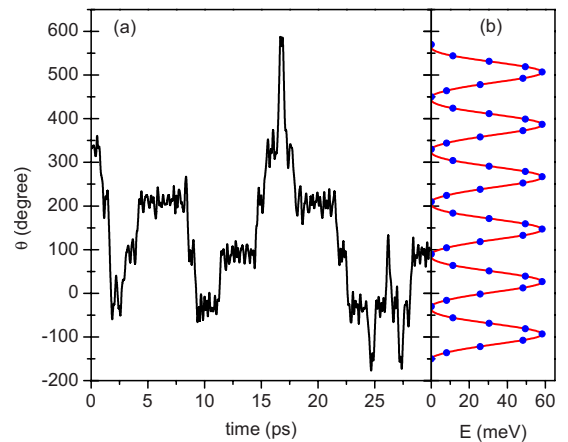


FIG. 3. (Color online) (a) The evolution of geometrical parameters in-plane angle  $\theta$  for MD simulation at 300 K for  $(2 \times 2)$ -2NO(fcc+top)/Pt(111). (b) Corresponding potential energy surface for the rotation ( $\theta$ ) of top NO from NEB calculations.

specific azimuth angle, in contrast to top NO in  $p(2 \times 2)$ -3NO(fcc+hcp+top) on Pd(111) at temperature even as lower as 140 K (Fig. 2). Actually, there is no rotation found for top NO in the given simulation time at 140 K.

#### IV. SUMMARY

Using DFT calculations at absolute zero and *ab initio* MD simulations at finite temperatures, NO adsorption on Pd(111) and Pt(111) surfaces were studied, and the interplay between the electronic interactions, lateral interactions and the effect of temperature on geometries were highlighted. We found that the electronic interactions was dominated at low coverage, where the hollow NO prefers the upright configuration, and the top NO prefers the tilting configuration. With increase in the coverage, the lateral interactions occurs, and

hollow NO becomes tilting too. We found that the effects of temperature on the geometries including the bond length and molecule orientations are significant. With the increase in temperature, the  $d_{N-metal}$  stretching and the tilting of NO molecule are enhanced. For top NO on Pd(111) and Pt(111) at 0.75 ML, there are no preferential tilting direction. However, for NO adsorption on Pt(111) at 0.50 ML, top NO prefers to tilt the fcc site nearby.

#### ACKNOWLEDGMENTS

W.X.L. thanks financial support from Natural Science Foundation of China (Grants No. 20733008 and No. 20873142) and National Basic Research Program of China (Grant No. 2007CB815205). J.L.F. Da Silva thanks the São Paulo Science Foundation (FAPESP).

- 
- <sup>1</sup>J. Kaspar, P. Fornasiero, and N. Hickey, *Catal. Today* **77**, 419 (2003).
- <sup>2</sup>J. K. Nørskov, T. Bligaard, J. Rossmeisl, and C. H. Christensen, *Nat. Chem.* **1**, 37 (2009).
- <sup>3</sup>R. B. Getman and W. F. Schneider, *J. Phys. Chem. C* **111**, 389 (2007).
- <sup>4</sup>M. Gajdoš, J. Hafner, and A. Eichler, *J. Phys.: Condens. Matter* **18**, 13 (2006).
- <sup>5</sup>D. C. Ford, Y. Xu, and M. Mavrikakis, *Surf. Sci.* **587**, 159 (2005).
- <sup>6</sup>H. Tang and B. L. Trout, *J. Phys. Chem. B* **109**, 17630 (2005).
- <sup>7</sup>R. Burch, S. T. Daniells, and P. Hu, *J. Chem. Phys.* **117**, 2902 (2002).
- <sup>8</sup>Q. Ge and D. A. King, *Chem. Phys. Lett.* **285**, 15 (1998).
- <sup>9</sup>W. A. Brown and D. A. King, *J. Phys. Chem. B* **104**, 2578 (2000).
- <sup>10</sup>Z.-H. Zeng, J. L. F. Da Silva, H.-Q. Deng, and W.-X. Li, *Phys. Rev. B* **79**, 205413 (2009).
- <sup>11</sup>K. H. Hansen, Ž. Šljivančanin, B. Hammer, E. Lægsgaard, F. Besenbacher, and I. Stensgaard, *Surf. Sci.* **496**, 1 (2002).
- <sup>12</sup>H. Aizawa, Y. Morikawa, S. Tsuneyuki, K. Fukutani, and T. Ohno, *Surf. Sci.* **514**, 394 (2002).
- <sup>13</sup>P. Kostelník, T. Šíkola, P. Varga, and M. Schmid, *J. Phys.: Condens. Matter* **21**, 134005 (2009).
- <sup>14</sup>M. Matsumoto, N. Tatsumi, K. Fukutani, and T. Okano, *Surf. Sci.* **513**, 485 (2002).
- <sup>15</sup>P. Zhu, T. Shimada, H. Kondoh, I. Nakai, M. Nagasaka, and T. Ohta, *Surf. Sci.* **565**, 232 (2004).
- <sup>16</sup>Z.-H. Zeng, J. L. F. Da Silva, and W.-X. Li, *Phys. Chem. Chem. Phys.*, doi:10.1039/B920857G (2010).
- <sup>17</sup>R. T. Vang, J. G. Wang, J. Knudsen, J. Schnadt, E. Laegsgaard, I. Stensgaard, and F. Besenbacher, *J. Phys. Chem. B* **109**, 14262 (2005).
- <sup>18</sup>J. P. Perdew, K. Burke, and M. Ernzerhof, *Phys. Rev. Lett.* **77**, 3865 (1996).
- <sup>19</sup>P. E. Blöchl, *Phys. Rev. B* **50**, 17953 (1994).
- <sup>20</sup>G. Kresse and D. Joubert, *Phys. Rev. B* **59**, 1758 (1999).
- <sup>21</sup>M. Marsman and G. Kresse, *J. Chem. Phys.* **125**, 104101 (2006).
- <sup>22</sup>G. Kresse and J. Hafner, *Phys. Rev. B* **48**, 13115 (1993).
- <sup>23</sup>G. Kresse and J. Furthmüller, *Phys. Rev. B* **54**, 11169 (1996).
- <sup>24</sup>C. Kittel, *Introduction to Solid State Physics*, 7th ed. (Wiley & Sons, New York, 1996).
- <sup>25</sup>H. Jonsson, G. Mills, and K. W. Jacobsen, *Classical and Quantum Dynamics in Condensed Phase Simulations* (World Scientific, Singapore, 1998).
- <sup>26</sup>G. Henkelman, B. P. Uberuaga, and H. Jonsson, *J. Chem. Phys.* **113**, 9901 (2000).
- <sup>27</sup>G. Henkelman and H. Jonsson, *J. Chem. Phys.* **113**, 9978 (2000).
- <sup>28</sup>D. Sheppard, R. Terrell, and G. Henkelman, *J. Chem. Phys.* **128**, 134106 (2008).
- <sup>29</sup>J. Paier, M. Marsman, K. Hummer, G. Kresse, I. C. Gerber, and J. G. Angyan, *J. Chem. Phys.* **124**, 154709 (2006).
- <sup>30</sup>J. F. Zhu, M. Kinne, T. Fuhrmann, B. Trankenschuh, R. De-necke, and H. P. Steinrck, *Surf. Sci.* **547**, 410 (2003).